



Cite this: *Sustainable Food Technol.*,  
2026, 4, 1883

## Valorization of chicken byproducts for bioactive coatings to extend the shelf life of okra (*Abelmoschus esculentus*)

Aparna Ramadoss,<sup>1</sup> Venkata Giridhar Poosarla,<sup>1</sup>\* Ananya Kumari, Shaik Sadiya,<sup>1</sup> Manisha Kalita and Nagaveni Shivshetty<sup>1</sup>

Environmental concerns associated with petroleum-based packaging have led to the development of sustainable alternatives and active packaging solutions. The aim of this research is to formulate and characterize bioactive packaging films based on pectin (P, 2%), sodium alginate (SA, 1.5%), and varying concentrations of chicken byproducts protein hydrolysates (CBP-PHs) that are derived from the enzymatic hydrolysis of CBPs using protease generated from *Bacillus siamensis* F2 and extend the shelf life of okra using coatings. The films F1, P + SA; F2, P + SA + 1%CBP-PHs; F3, P + SA + 1.5%CBP-PHs; and F4, P + SA + 2%CBP-PHs were analyzed for physical, antibacterial, antioxidant, and structural properties. Among them, the F4 film showed the highest antioxidant (diphenylpicrylhydrazyl,  $53 \pm 0.75\%$ ), antibacterial (*Staphylococcus aureus*,  $24.5 \pm 0.16$  mm and *Klebsiella pneumoniae*,  $21 \pm 0.12$  mm), and surface hydrophobicity ( $132^\circ$ ) properties due to the highest concentration of CBP-PHs. Based on this, F4 film coatings were applied to okra to evaluate their ability to extend shelf life, and F1-coating and uncoated okra were used as controls. F4-coated okra exhibited lower weight loss ( $78 \pm 0.4\%$ ), chlorophyll loss, and ascorbic acid ( $7.6 \pm 0.1$  mg/100 g), while effectively retaining firmness ( $51 \pm 0.8$  N) and color. These findings highlight the potential of CBP-PH-impregnated active coatings as a sustainable alternative with excellent shelf life extension, supporting the development of green packaging technology that aligns with global sustainability goals. Future research will aim to optimize F4 film formulation for commercial production and investigate its application on various perishable products.

Received 9th August 2025  
Accepted 16th December 2025

DOI: 10.1039/d5fb00468c

rsc.li/susfoodtech

### Sustainability spotlight

Protein hydrolysates (PHs) obtained from chicken byproducts (CBPs) via enzymatic hydrolysis using *Bacillus siamensis* F2 protease were incorporated into a pectin and sodium alginate (SA) biopolymer matrix to fabricate active packaging films. These films exhibited strong antimicrobial and antioxidant properties, and the active coatings extended the postharvest shelf life of okra. This study valorises poultry byproducts into functional coatings that substitute petroleum-based polymers. Such coatings reduce food waste and advance sustainable packaging technologies aligned with the United Nations Sustainable Development Goals (SDGs) – 2, 3, 6, 9, 14, and 15, specifically targeting SDG-2 (End hunger, achieve food security, and improved nutrition). Ultimately, this study enhances food security by transforming poultry byproducts into value-added resources for sustainable packaging.

## 1 Introduction

Biodegradable packaging is a sustainable alternative to conventional packaging, offering biodegradability, biocompatibility, and aesthetic appeal, and facilitates the protection and transport of food.<sup>1,2</sup> Active packaging integrates compounds that absorb or release components from packed food or the surrounding environment. They effectively preserve food safety, quality, and sensory characteristics while enhancing shelf life.<sup>3</sup> Various materials have been studied for active packaging;

however, the focus has shifted towards naturally derived polymers like polysaccharides (cellulose, starch, pectin, and alginate), proteins (sodium caseinate, whey protein, soy protein, corn zein, and gelatin), and nanoparticles.<sup>4</sup>

Among biopolymers, alginate is a linear copolymer that comprises  $\beta$ -D-mannuronic acid (M) residues and  $\alpha$ -L-guluronic acid (G), arranged in homopolymeric (GG and MM) and heteropolymeric (MG) block sequences. They are naturally derived polysaccharides extracted from brown algae (*Phaeophyceae*), typically found as sodium, calcium, or magnesium salts of alginic acid.<sup>5</sup> Alginate offers good film formation, flexibility, water solubility, tear resistance, tensile strength, rigidity, low water vapor and oxygen permeability, and a neutral taste and odor. Enriched with essential oils, proteins, enzymes,

Department of Life Sciences, GITAM School of Science, GITAM (Deemed to be University), Visakhapatnam, Andhra Pradesh, 530045, India. E-mail: gpoosarl@gitam.edu



chelating agents, plant extracts, or metallic nanoparticles, they help retain moisture, reduce shrinkage and oxidation, and preserve color and texture. It enhances the antimicrobial activity, mechanical strength, barrier performance, and sensory quality while minimizing cooking losses.<sup>6</sup>

Pectin has excellent gelling and thickening properties and a distinct flavour, making it valuable in food packaging. It reduces the environmental footprint of conventional packaging, minimizing the use of hazardous substances, reducing food spoilage, and ultimately improving shelf life and food quality.<sup>7,8</sup> To further optimize the performance of polysaccharides such as alginates, pectin, and biocomposites, recent research is exploring incorporating protein hydrolysates (PHs) to produce active packaging films. This innovative strategy utilises protein byproducts to improve sustainability.<sup>9,10</sup>

Protease enzymes are essential for producing peptides and amino acids by hydrolysing proteins. This releases bioactive substances and improves the valorisation of protein-rich byproducts. Several commercial proteases, such as Flavourzyme®, Pancreas Trypsin®, Alcalase®, and Novo ProD®, are used to produce hydrolysates with antioxidant activity (AA) and emulsifying properties.<sup>11</sup> Microbial proteases have emerged as cost-effective, highly specific, and sustainable alternatives, offering excellent stability under extreme conditions, such as high salinity and pH, making them suitable for industrial protein hydrolysis.<sup>12–15</sup> The resulting PHs, composed of peptides of varying lengths, exhibit modified structures that influence their physicochemical and functional properties.

Studies have demonstrated the strong potential of bioactive film development for packaging, offering enhanced antimicrobial, antioxidant, barrier, and mechanical properties, which leads to the extension of food shelf life.<sup>16,17</sup> Recent studies have shown that PHs derived from poultry demonstrate superior AA, barrier properties, and antimicrobial activity against *Escherichia coli* and *Staphylococcus saprophyticus*.<sup>10,16</sup> These PHs also extended the shelf life of sweet cherry at both room temperature and under refrigerated conditions.<sup>10</sup> Similarly, incorporation of fish PHs has been reported to extend the shelf life of chicken fillets to 21 days.<sup>17</sup>

Okra (*Abelmoschus esculentus*), a nutritionally rich crop with a high water content (85%), consists of non-cellulosic and non-starch polysaccharides. It possesses several nutritional properties and serves as a source of vitamins A and C, proteins, calcium, iron, dietary fiber, and antioxidants. It helps lower serum cholesterol, thereby minimizing the risk of cardiovascular diseases, digestive disorders, and type 2 diabetes. Due to its high moisture content and respiration rate, okra is highly perishable and prone to rapid quality deterioration. It is particularly susceptible to water loss, discolouration, and textural degradation, which significantly reduces its commercial value. Therefore, effective preservation strategies are crucial for minimizing postharvest losses, preventing food waste, and contributing to improved food security.<sup>18–20</sup>

Several studies have investigated the development of packaging films using individual components such as sodium alginate (SA), pectin (P), and protein hydrolysates (PHs) from various sources. The research gap is to generate PHs from

chicken byproducts (CBPs) using the protease of *Bacillus siamensis* F2 isolated in our laboratory and explore its potential as a functional component to extend the shelf life of okra. This research aims to impregnate chicken byproducts protein hydrolysates (CBP-PHs) into a P and SA matrix to produce active films. They were characterized for their physical, optical, antioxidant, antibacterial and structural properties. This film formulation was applied as a coating to okra to evaluate its ability to extend shelf life by studying parameters such as weight loss, pH, firmness, ascorbic acid content, antioxidant activity, color, and microbial analysis. These findings offer an innovative, eco-friendly solution for sustainable packaging and contribute to Sustainable Development Goal 2 (Zero Hunger) by valorising CBPs and reducing food spoilage.

## 2 Materials and methods

### 2.1 Materials

Extrapure SA (sodium polymannuronate) (Finar, Gujarat, India), pure pectin (high methoxyl content (7%) and a minimum of 50% galacturonic acid) and 2,2-diphenyl-1-picrylhydrazyl (DPPH) (Sisco research laboratory, Maharashtra, India), calcium chloride (CaCl<sub>2</sub>) (Emparta, Mumbai, India), glycerol (Qualigens, Maharashtra, India), and Muller Hinton agar (HiMedia, Maharashtra, India) were purchased. Chicken byproducts (CBPs) were obtained from a local poultry slaughterhouse, and okra was sourced from a local vegetable market in Visakhapatnam, India. According to our previous studies, the bacterium *Bacillus siamensis* F2<sup>21</sup> was isolated from the water of a fish processing plant in Visakhapatnam, India, and the protease produced by this bacterium F2 was optimized and characterized.<sup>13</sup> After obtaining promising results, this F2 protease (5.2 U mL<sup>-1</sup>)<sup>13</sup> was used to produce CBP-PHs using CBPs to make active packaging films.

### 2.2 Preparation of active films

The active packaging films were developed using the solvent casting method accordingly<sup>8,22</sup> with slight modifications. Pectin (2 g) and SA (1.5 g) were added to distilled water (DW) (0.1 L) and heated for 25–30 min at 60 °C on a hot plate. This solution was brought to room temperature, and CBP-PHs, extracted accordingly,<sup>13</sup> were incorporated in varying concentrations (1, 1.5, and 2%) with glycerol (2%) as a plasticizer. The obtained solution was transferred into a Petri plate (145 mm diameter) and left for drying in a biological oxygen demand (Model-925100, Labocare, India) at 30 °C. Once the films had dried, they were carefully peeled off and kept in an incubator at 35 °C for further analysis. After peeling the films off the casting plates, the dried films were labelled as F1, P + SA; F2, P + SA + 1%CBP-PHs; F3, P + SA + 1.5%CBP-PHs; and F4, P + SA + 2%CBP-PHs, as shown in Fig. 1.

### 2.3 Characterization of films

#### 2.3.1 Physical properties

**2.3.1.1 Thickness.** A digital Vernier caliper (Mitutoyo Absolute, range: 0–150 mm) with a least count of 0.00 mm at three



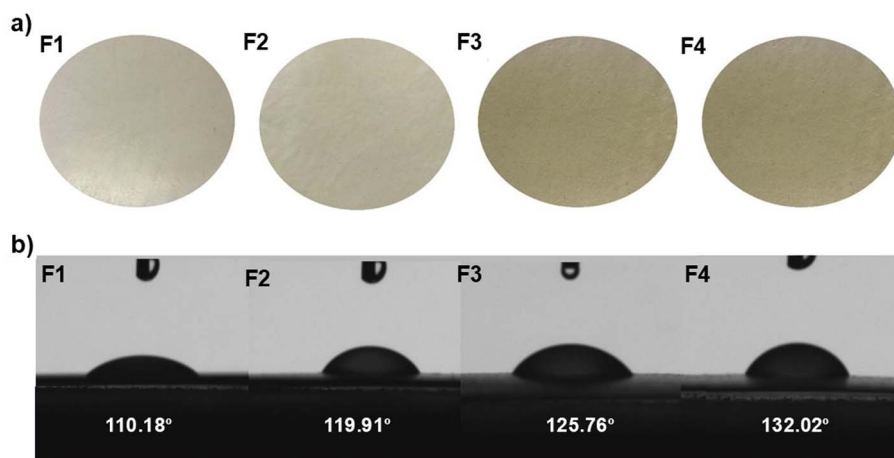


Fig. 1 (a) Preparation of active packaging films. (b) Contact angle values of different films. F1, P + SA; F2, P + SA + 1%CBP-PHs; F3, P + SA + 1.5% CBP-PHs; and F4, P + SA + 2%CBP-PHs. P, pectin; SA, sodium alginate; CBP-PHs, chicken byproducts protein hydrolysates.

random points was used to measure the thickness of the developed films.<sup>22</sup>

**2.3.1.2 Moisture content (MC).** The initial and final weights of the developed films ( $2 \times 2 \text{ cm}^2$ ) were recorded before and after drying at  $105 \text{ }^\circ\text{C}$  for 3 h in a hot air oven.<sup>22</sup> MC was calculated using eqn (1):

$$\text{Moisture content(\%)} = \frac{W_i - W_f}{W_i} \times 100 \quad (1)$$

where  $W_i$  is the initial weight before drying and  $W_f$  is the final weight after drying.

**2.3.1.3 Water solubility (WS).** The film samples ( $2 \times 2 \text{ cm}^2$ ) were weighed, placed in 10 mL of DW, and kept in a shaking incubator (Model-1254504, Venchal Scientific, India) at 180 rpm for 24 h. This solution was centrifuged at 1500 rpm for 20 min, and the undissolved pellet was dehydrated at  $105 \text{ }^\circ\text{C}$  for 24 h using a hot air oven and then weighed.<sup>22</sup> The WS was calculated by using eqn (2):

$$\text{Water solubility(\%)} = \frac{W_1 - W_2}{W_1} \times 100 \quad (2)$$

where  $W_1$  is the initial weight of the film before drying and  $W_2$  is the final weight of the dried film.

**2.3.1.4 Swelling index (SI).**  $2 \times 2 \text{ cm}^2$  film samples were weighed and placed in 25 mL of DW for 2 min. Then, the surface water was discarded, and the films were reweighed.<sup>22</sup> The SI was calculated using eqn (3):

$$\text{Swelling index(\%)} = \frac{W_1 - W_2}{W_2} \times 100 \quad (3)$$

where  $W_1$  is the weight of the swollen film and  $W_2$  is the weight of the dry film.

**2.3.1.5 Water contact angle (WCA).** The WCA of the fabricated films was evaluated using a contact angle meter (Acam-HSC 19, Apex Instruments, Kolkata, India) using the sessile drop technique, accordingly with slight modifications.<sup>23</sup> A  $7 \text{ } \mu\text{L}$  DW was gently dispensed on the film surface using a glass

syringe at  $25 \text{ }^\circ\text{C}$  and 50% relative humidity, and the average of five replicates was reported.

**2.3.1.6 Density.** The developed active films were cut into  $4 \times 1 \text{ cm}^2$ , and the density was calculated using mass, area, and thickness<sup>22</sup> using eqn (4):

$$\text{Density}(\text{g cm}^{-3}) = \frac{M}{A \times d} \quad (4)$$

where  $M$  is the mass (g),  $A$  is the area ( $\text{cm}^2$ ), and  $D$  is the thickness of the film.

**2.3.1.7 Water vapor permeability (WVP).** WVP was used to determine the amount of water that diffuses within the film. The film was sealed on the mouth of the test tube containing anhydrous  $\text{CaCl}_2$ . Then, these sealed test tubes were kept in a desiccator at  $30 \text{ }^\circ\text{C}$  and 75% relative humidity.<sup>8</sup> The samples were weighed every 24 h until the weight change was 0.001 g using eqn (5):

$$\text{Water vapor permeability}(\text{g (m}^{-1} \text{ s}^{-1} \text{ Pa}^{-1})) = \frac{(m_1 - m_0)L}{At\Delta P} \quad (5)$$

where  $m_1$  and  $m_0$  are the final and the initial weights of the test tube, g;  $L$  is the thickness of the film, m;  $A$  is the area of the exposed film,  $\text{m}^2$ ;  $t$  is the time, s; and  $\Delta P$  is the water vapor pressure on either side of the film, Pa.

**2.3.2 Optical properties-transparency and opacity.** The opacity and transparency were determined using an ultraviolet-visible (UV-vis) spectrophotometer (Shimadzu UV-1800, Nakagyo-Ku, Kyoto, Japan) by cutting the films into rectangular strips ( $4 \times 1 \text{ cm}^2$ ) and measuring at 670 and  $800 \text{ nm}$ <sup>22</sup> using eqn (6) and (7):

$$\text{Opacity} = \frac{\text{Abs}_{670}}{x} \quad (6)$$

$$\text{Transparency} = \frac{\log(\% T_{800})}{x} \quad (7)$$



where  $Abs_{670}$  is the absorbance at 670 nm, %  $T_{800}$  is the transmittance at 800 nm, and  $x$  is the film thickness, mm.

### 2.3.3 Antioxidant activity

**2.3.3.1 Diphenylpicrylhydrazyl (DPPH) assay.** The AA of the developed films was determined by DPPH assay.<sup>22</sup> In 3 mL of DPPH (0.1 mM) solution, 6 mg of the film was immersed for 24 h, and the optical density was measured at 517 nm using a UV-vis spectrophotometer. The DPPH solution was taken as a control, and the AA of the film samples was calculated using eqn (8):

$$\text{Antioxidant activity(\%)} = \frac{\text{Ab control} - \text{Ab sample}}{\text{Ab control}} \times 100 \quad (8)$$

where Ab control is the absorbance value for the DPPH solution and Ab sample is the absorbance value for the film samples.

**2.3.3.2 Metal chelating activity (MCA).** The chelating activity of the biodegradable films on  $Fe^{2+}$  ions was determined.<sup>22</sup> 1 mL of the film solution was mixed with 3.7 mL of DW and maintained at room temperature. Then, 0.1 mL of 2 mM  $FeCl_2$  and 0.2 mL of 5 mM ferrozine [3-(2-pyridyl)-5,6-bis(4-phenyl-sulfonic acid)-1,2,4-triazine] were added. The mixture was incubated for 20 min, and the absorbance was measured at 562 nm using a UV-vis spectrophotometer. The chelating activity (%) was calculated using eqn (9), where 1 mL of DW served as the control.

$$\text{Metal chelating activity(\%)} = 1 - \frac{\text{Absorbance of sample at 562 nm}}{\text{Absorbance of control at 562 nm}} \times 100 \quad (9)$$

**2.3.3.3 Hydroxyl radical-scavenging activity (HRSA).** The hydroxyl radical-scavenging activity of the biodegradable films was determined.<sup>22</sup> Briefly, a mixture containing 0.75 mM 1,10-phenanthroline and 0.75 mM  $FeSO_4$  was prepared in 0.1 M phosphate buffer (pH 7.4) and mixed thoroughly. To this, 0.01%  $H_2O_2$  and the film solution (1.5 mg  $mL^{-1}$ ) were added, and the reaction mixture was incubated at 37 °C for 1 h. The absorbance of the resulting solution was measured at 536 nm using a UV-vis spectrophotometer. The scavenging activity was calculated using eqn (10).

$$\begin{aligned} \text{Hydroxyl radical - scavenging activity} \\ = 0.5 \times \left[ \frac{A_s - A_1}{A_0 - A_1} \right] \times 100 \end{aligned} \quad (10)$$

where  $A_s$  represents the absorbance of the sample,  $A_1$  represents the absorbance of the control solution containing 1,10-phenanthroline,  $FeSO_4$ , and  $H_2O_2$ , and  $A_0$  represents the absorbance of the blank solution containing 1,10-phenanthroline and  $FeSO_4$ .

**2.3.4 Antibacterial activity.** The antibacterial activity of films was assessed using the Kirby–Bauer disc diffusion assay. *Klebsiella pneumoniae* (ATCC 13883) and *Staphylococcus aureus* (ATCC 25923) inocula were standardized using McFarland standards ( $0.5 = 1.5 \times 10^8$  CFU  $mL^{-1}$ ) and swabbed onto Mueller–Hinton agar plates. A 1 cm film was placed on the plate and incubated at 37 °C for 24 h, and the zone of inhibition (ZOI) was measured.<sup>22</sup>

### 2.3.5 Liquid chromatography-mass spectrometry (LC-MS).

LC-MS of the CBP-PHs was performed to detect and identify the presence of bioactive peptides to confirm the film's antioxidant and antibacterial activity. Peptide detection was performed using a Waters XEVO G3 Quadrupole-Time-of-flight High-Resolution Mass Spectrometry (QToF HRMS) system (Waters Corporation, USA). Chromatographic separation was performed on an ACQUITY BEH C18 column (100 × 2.1 mm, 1.7 μm, 100 Å). The mobile phase consisted of (A) water containing 0.1% formic acid and (B) acetonitrile containing 0.1% formic acid. Nitrogen was used as the source gas, and argon served as the collision gas for collision-induced dissociation (CID). The spectral data were acquired in positive ion mode, with a  $m/z$  ratio ranging from 100 to 2000.<sup>24</sup>

### 2.3.6 Fourier transform infrared (FTIR) spectroscopy.

Functional groups were analysed using a Bruker Alpha-II Attenuated Total Reflectance-Fourier Transform Infrared (ATR-FTIR) spectrophotometer. The spectral data were collected over wavenumbers from 4000 to 500  $cm^{-1}$ . Each sample underwent 80 scans with a scanning resolution set at 4  $cm^{-1}$  using a zinc selenide beam splitter, and the data were processed using the software OPUS 7.1.<sup>8</sup>

**2.3.7 X-ray diffraction (XRD).** XRD analysis was performed employing an XRD device (Bruker D8 Advance, USA) using  $Cu K\lambda$  radiation ( $\lambda = 1.5406 \text{ \AA}$ ) with a  $0.02^\circ$  increment of 2 s per step, 40 kV voltage, and current of 40 mA, ranging from 5 to  $70^\circ$ .<sup>8</sup>

## 2.4 Shelf life studies

Shelf life refers to the duration a product remains suitable for use. *Abelmoschus esculentus*, commonly known as okra, was chosen for this shelf life study because it is highly perishable. It is a highly nutritious crop that can lose its quality due to respiration and moisture loss through transpiration after harvest.<sup>25</sup>

**2.4.1 Formulation of the coating solution.** The coating formulation included pectin (2%), SA (1.5%) and CBP-PHs of F1 (0%) and F4 (2%).

**2.4.2 Application of coating on okra.** Shelf life studies using okra were conducted to evaluate the distinctive qualities of the newly developed active film. Okra is a nutrient-rich crop that suffers from significant losses during storage.<sup>26</sup> On March 10, 2025, 174 okras were acquired from a local grocery market in Visakhapatnam, India. The chosen pods were uniform in size, maturity, and color and free from microbial contamination. The pods were washed with 2% sodium hypochlorite, followed by DW, and dried at 37 °C. Then, they were randomly divided into three groups with 58 each and treated with the coating solution using a dipping and cross-polymerization method that utilized  $CaCl_2$ .<sup>19</sup> Approximately 210 mL of the film-forming solution was used to coat the 116 okras (1.8 mL per pod), whereas 90 mL of the film-forming solution was used to wrap only two okras; hence, dip-coating was selected over wrapping with films. After coating, the samples were dried and stored at room temperature (30 °C) for further analysis. A comprehensive analysis was conducted across all groups to evaluate the final quality



attributes, with a primary focus on weight loss, pH, firmness, ascorbic acid content, total chlorophyll content, color, and microbial analysis. This systematic approach aims to ascertain the efficiency of CBP-PHs in enhancing the storage of okra, contributing to understanding the efficiency of active film application in food preservation.<sup>26</sup>

**2.4.3 Weight loss.** The weight loss of okra was determined using the initial weight ( $W_i$ ) (day 0) and final weight ( $W_f$ ) (day of analysis) difference of the samples using a precision balance (Venchal Scientific),<sup>26</sup> using eqn (11):

$$\text{Weight loss (\%)} = \frac{W_i - W_f}{W_i} \times 100 \quad (11)$$

**2.4.4 pH.** pH was determined using a digital pH meter (ESICO 1010). Whole okras were used after removing the seeds and were homogenized using a blender, and the electrode probe of the pH meter was inserted to observe the pH.<sup>19</sup>

**2.4.5 Firmness.** The firmness of okra was determined with a texture analyzer (TA-CT3, Brookfield Engineering Laboratories, Inc., MA, USA) to investigate the textural characteristics of the okra. The okra sample was placed on the base of the analyzer, and force was applied using a cylindrical probe with a 2 mm radius. The test parameters were as follows: 5 N trigger force, 2 mm s<sup>-1</sup> test speed, 5 mm s<sup>-1</sup> pre-test speed, 2 mm s<sup>-1</sup> post-test speed, and 25% strain deformation. The dual compression method was employed, with a 5-second interval maintained between the two compression cycles of the samples.<sup>27</sup>

**2.4.6 Ascorbic acid.** The ascorbic acid content of the okra was determined using a 5 mL solution of 100 µg mL<sup>-1</sup> ascorbic acid in oxalic acid as a standard. 5 mL of 100 µg mL<sup>-1</sup> ascorbic acid was added to 10 mL of 4% oxalic acid and titrated against the dye (42 mg of sodium bicarbonate was mixed with 52 mg of 2, 6-dichlorophenol indophenol and made up to 200 mL using DW) ( $V_1$ ) until the pink color persisted. 5 g of the okra sample was dissolved in 80 mL of 4% oxalic acid and brought to a volume of 100 mL. The mixture was then centrifuged, and 5 mL of the supernatant was added to 10 mL of 4% oxalic acid and titrated against the dye ( $V_2$ ).<sup>28</sup> The amount of ascorbic acid in the sample was calculated using eqn (12):

$$\begin{aligned} \text{Ascorbic acid (mg/100 g)} &= \frac{0.5 \text{ mg}}{V_1 \text{ mL}} \times \frac{V_2 \text{ mL}}{5 \text{ mL}} \\ &\times \frac{100 \text{ mL}}{\text{Weight of the sample}} \times 100 \end{aligned} \quad (12)$$

**2.4.7 Antioxidant activity.** The AA of okra was determined by the DPPH assay accordingly with slight modifications.<sup>29</sup> 50 µL of okra extract was mixed with 250 µL of 0.1 mM methanolic DPPH solution and incubated in the dark at room temperature for 1 h. The absorbance was measured at 517 nm and the AA was calculated using eqn (13):

$$\text{Antioxidant activity (\%)} = \frac{\text{Ab control} - \text{Ab sample}}{\text{Ab control}} \times 100 \quad (13)$$

**2.4.8 Color.** The color parameters for okra were measured using a HunterLab colorimeter (ColorFlex EZ, USA)<sup>30</sup> based on the International Commission on Illumination (CIE)  $L^*$ ,  $a^*$ , and  $b^*$  system with the illuminant D65 and a standard observer of 10°. The colorimeter was calibrated using a white and black standard calibration plate. The black to white was indicated by  $L^*$ , red (positive) to green (negative) by  $a^*$ , and yellow (positive) to blue (negative) by  $b^*$ .<sup>31</sup> The Browning index (BI) of okra was also calculated using eqn (14) and (15):

$$\text{Browning index (BI)} = \frac{[100(x - 0.31)]}{0.17} \quad (14)$$

$$x = \frac{a^* + 1.75 L^*}{5.645 L^* + a^* - 3.012 b^*} \quad (15)$$

**2.4.9 Total chlorophyll content.** Total chlorophyll content was quantified by homogenizing 3 g of okra with 10 mg of magnesium sulphate ( $\text{MgSO}_4$ ) and 30 mL of 80% acetone using a mortar and pestle. Then, the solution was filtered and quantified in a 50 mL volumetric flask. The absorbance of the extract was measured at 663 and 645 nm using a UV-vis spectrophotometer<sup>32</sup> and calculated using eqn (16):

$$\begin{aligned} \text{Total chlorophyll content (mg/100 g)} \\ = \frac{(20.2 \times \text{Abs}_{645}) + (8.02 \times \text{Abs}_{663}) \times 50 \times 100}{1000 \times \text{weight of sample}} \end{aligned} \quad (16)$$

where  $\text{Abs}_{645}$  is the absorbance at 645 nm and  $\text{Abs}_{663}$  is the absorbance at 663 nm.

**2.4.10 Total microbial count.** The microbial count was determined using the pour plate technique, employing nutrient agar (NA) for bacterial counts and yeast extract peptone dextrose (YEPD) for yeast and mold counts, both of which were performed using the serial dilution technique. 1 mL of the okra sample was added to 9 mL of 0.1% sterile peptone water. From this homogenized sample, a 1 mL aliquot was transferred into sterile Petri plates, and molten NA and YEPD were gently poured. The plates were gently swirled to ensure uniform mixing, and then the agar plates were incubated for 2 days at 37 °C (NA) and 5 days at 25 °C for YEPD. The microbial growth was expressed as the logarithm of colony-forming units per gram ( $\log \text{CFU g}^{-1}$ ).<sup>8</sup>

## 2.5 Statistics

The statistical analysis was conducted using OriginPro 8.5. One-way ANOVA, followed by Tukey's Honestly Significant Difference (HSD) test, and two-way ANOVA, followed by the Bonferroni test, were used to evaluate differences between group means. All the analyses were conducted in triplicate, and the results were considered statistically significant at  $p < 0.05$ . Pearson correlation was performed to assess the physical, optical, antioxidant, and antibacterial properties of the films.



### 3 Results and discussion

In this study, CBP-PHs were extracted from CBPs using the protease of the bacterium *Bacillus siamensis* F2 (5.2 U mL<sup>-1</sup>) accordingly.<sup>13</sup> The produced CBP-PHs were impregnated in a pectin and SA matrix to produce active packaging films. The produced active films are characterized and applied to food as a coating to monitor their ability to extend shelf life.

#### 3.1 Developed films

The films were developed using pectin (P) (2%), sodium alginate (SA) (1.5%), and CBP-PHs of varying composition – F1, P + SA; F2, P + SA + 1%CBP-PHs; F3, P + SA + 1.5%CBP-PHs; and F4, P + SA + 2%CBP-PHs (Fig. 1). The pH of the developed film forming solutions was measured as follows – F1 (4.2), F2 (4.31), F3 (4.36), and F4 (4.4).

#### 3.2 Film characterization

**3.2.1 Thickness.** The thickness of the developed film increased with the concentration of CBP-PHs from 0.32 ± 0.015 mm (F1) to 0.42 ± 0.005 mm (F4) (Table 1). This increase resulted from incorporating the CBP-PHs into the SA and pectin matrix, which enhanced the overall solid content of the film. The increase in the dissolved solid components contributed to stronger intermolecular interactions and molecular spacing within the film's structure, resulting in a thicker structure.<sup>10,33,34</sup> A similar increase in thickness from 0.12 to 0.23 mm was observed when 1.5% alginate was incorporated with varying concentrations of cottonseed PHs (0, 0.15, 0.3, and 0.6%).<sup>33</sup> Another study also demonstrated a similar increase in thickness with the addition of hydrolysates.<sup>35</sup>

**3.2.2 Moisture content (MC), water solubility (WS), swelling index (SI), and water contact angle (WCA).** The MC, WS, and SI decrease with an increased CBP-PH concentration (Table 1). The control film F1 (without CBP-PHs) shows a higher MC of 22 ± 0.19% compared to F2, F3, and F4 (19 ± 0.47, 18 ± 0.43, and 16 ± 0.32% respectively). The WS decreases from 74 ± 0.5% in the F1 film to 57 ± 0.26% in the F4 film, and the SI decreases from 486 ± 1.09% (F1) to 372 ± 0.29% (F4). This occurred due to the linear polysaccharides, such as SA and pectin, forming moderate branching and covalent bonds with polyvalent metal cations

(magnesium, calcium, iron, *etc.*) present in CBP-PHs. The agglomerate formed increases the water resistance of the films by narrowing the distance between molecules, thereby forming a three-dimensional dense network. This enhances film stability in water by restricting water penetration and increasing surface hydrophobicity.<sup>10,36,37</sup> A similar decrease in WS from 84 to 60% was observed when 3% maize starch was incorporated with varying concentrations of chicken feather PHs (0, 1.5, 3, and 6%).<sup>38</sup> Similarly, another study observed a decreasing trend of the SI from 570 to 328% when a fish gelatin film was impregnated with liquid fish hydrolysate.<sup>37</sup>

As the concentration of CBP-PHs increases from 0 to 2% in the films, the WCA of the films shows an increase from 110° to 132°, demonstrating hydrophobicity (Fig. 1b). The films containing pectin and SA form an agglomerate when CBP-PHs are added, thereby increasing water resistance by forming a dense matrix.<sup>10,36,37</sup> This imparts moisture resistance, leading to higher surface hydrophobicity, an increased contact angle, and reduced wettability.<sup>39</sup> A similar increase in hydrophobicity was observed in a study where the contact angle increased from 68° to 96° with the addition of whitecheek shark PHs in whitecheek shark gelatin films.<sup>23</sup> Another study also observed a similar increase in hydrophobicity in SA films with the addition of gold-titanium dioxide nanoparticles.<sup>40</sup>

**3.2.3 Density.** The density progressively increased from 0.1 ± 0.001 g cm<sup>-3</sup> in the control F1 film to 0.13 ± 0.001 g cm<sup>-3</sup> in the F4 film due to the increased CBP-PH concentration (Table 1). This increasing trend can be attributed to the addition of the active component, CBP-PHs, to the pectin and SA matrix, which enhances aggregation and increases the overall solid content. Moreover, the presence of dissolved solids promoted stronger intermolecular interactions and greater molecular packing within the film structure, thereby increasing the film's volume and density.<sup>10,33,34</sup> A similar increase in density was observed when the SA and active components, quercetin and *Vitis vinifera* leaf extracts, were impregnated in the film matrix.<sup>41</sup> Another study also observed a similar increasing trend where the density of SA films increased from 0.045 to 0.056 g cm<sup>-3</sup> with the incorporation of fish PHs.<sup>17</sup>

**3.2.4 Water vapor permeability (WVP).** The WVP of the developed bioactive films increased by incorporating CBP-PHs

Table 1 Physical and optical properties of the developed films<sup>a</sup>

Parameters	F1	F2	F3	F4
Density (g cm <sup>-3</sup> )	0.10 ± 0.001 <sup>a</sup>	0.11 ± 0.005 <sup>b</sup>	0.12 ± 0.002 <sup>c</sup>	0.13 ± 0.001 <sup>d</sup>
Moisture content (%)	22.37 ± 0.19 <sup>a</sup>	19.48 ± 0.47 <sup>b</sup>	18.18 ± 0.43 <sup>c</sup>	15.92 ± 0.32 <sup>d</sup>
Opacity (%)	0.3 ± 0.001 <sup>a</sup>	0.36 ± 0.002 <sup>b</sup>	0.43 ± 0.003 <sup>c</sup>	0.54 ± 0.008 <sup>d</sup>
Swelling index (%)	485.7 ± 1.09 <sup>a</sup>	450.5 ± 0.25 <sup>b</sup>	416.9 ± 0.05 <sup>c</sup>	372.1 ± 0.29 <sup>d</sup>
Transparency (%)	5.54 ± 0.017 <sup>a</sup>	5.21 ± 0.05 <sup>b</sup>	4.82 ± 0.01 <sup>c</sup>	4.42 ± 0.02 <sup>d</sup>
Thickness (mm)	0.32 ± 0.015 <sup>a</sup>	0.35 ± 0.01 <sup>b</sup>	0.39 ± 0.005 <sup>c</sup>	0.42 ± 0.005 <sup>d</sup>
Water solubility (%)	74.11 ± 0.5 <sup>a</sup>	64.81 ± 0.8 <sup>b</sup>	61.44 ± 0.56 <sup>c</sup>	57.48 ± 0.26 <sup>d</sup>
WVP (10 <sup>-8</sup> g (m <sup>-1</sup> s <sup>-1</sup> Pa <sup>-1</sup> ))	1.99 ± 0.07 <sup>a</sup>	2.14 ± 0.05 <sup>b</sup>	2.3 ± 0.01 <sup>c</sup>	2.5 ± 0.02 <sup>d</sup>

<sup>a</sup> F1, P + SA; F2, P + SA + 1% CBP-PHs; F3, P + SA + 1.5%CBP-PHs; and F4, P + SA + 2%CBP-PHs. P, pectin; SA, sodium alginate; CBP-PHs, chicken byproducts protein hydrolysates; WVP, water vapor permeability. All data are averages of three measurements and reported as mean ± standard deviation (SD). Different letters (a, b, c, and d) indicate significant differences between groups at *p* < 0.05 according to Tukey's honestly significant difference (HSD) test.



Table 2 Antioxidant activity of the developed films<sup>a</sup>

Parameters	F1	F2	F3	F4	Ascorbic acid standard
DPPH (%)	39.2 ± 0.3 <sup>a</sup>	46.26 ± 0.7 <sup>b</sup>	48.42 ± 0.6 <sup>c</sup>	52.87 ± 0.75 <sup>d</sup>	92 ± 1.32 <sup>e</sup>
MCA (%)	21.3 ± 0.4 <sup>a</sup>	31.1 ± 0.2 <sup>b</sup>	36.4 ± 0.5 <sup>c</sup>	44.5 ± 0.7 <sup>d</sup>	82 ± 0.75 <sup>e</sup>
HRSA (%)	24.1 ± 0.2 <sup>a</sup>	31.7 ± 0.3 <sup>b</sup>	39.4 ± 0.4 <sup>c</sup>	48.5 ± 0.5 <sup>d</sup>	86 ± 0.87 <sup>e</sup>

<sup>a</sup> F1, P + SA; F2, P + SA + 1%CBP-PHs; F3, P + SA + 1.5%CBP-PHs; and F4, P + SA + 2%CBP-PHs. P, pectin; SA, sodium alginate; CBP-PHs, chicken byproducts protein hydrolysates. DPPH, diphenylpicrylhydrazyl; MCA, metal chelating activity; HRSA, hydroxyl radical-scavenging activity. All data are averages of three measurements and reported as mean ± standard deviation (SD). Different letters (a, b, c, and d) indicate significant differences between groups at  $p < 0.05$  according to Tukey's honestly significant difference (HSD) test.

(Table 1). The control film formulation, F1, without CBP-PHs, demonstrated the lowest WVP value of approximately  $2 \times 10^{-8} \pm 0.07 \times 10^{-8} \text{ g (m}^{-1} \text{ s}^{-1} \text{ Pa}^{-1})$ , whereas WVP increased subsequently in F2 ( $2.1 \times 10^{-8} \pm 0.05 \times 10^{-8} \text{ g (m}^{-1} \text{ s}^{-1} \text{ Pa}^{-1})$ ), followed by F3 ( $2.3 \times 10^{-8} \pm 0.01 \times 10^{-8} \text{ g (m}^{-1} \text{ s}^{-1} \text{ Pa}^{-1})$ ), and finally F4 ( $2.5 \times 10^{-8} \pm 0.02 \times 10^{-8} \text{ g (m}^{-1} \text{ s}^{-1} \text{ Pa}^{-1})$ ), with 1, 1.5, and 2% CBP-PHs respectively. The increase in WVP can be attributed to the increased thickness of the CBP-PH films and the plasticization effect of the peptides present in CBP-PHs. This increases the film matrix's free volume, making the matrix's network less dense and thereby increasing the water diffusion rate into the CBP-PH films.<sup>33,42</sup> The results align with a previous study where the WVP increases from  $6.3 \times 10^{-5} \text{ g mm m}^{-2}$  to  $10.9 \times 10^{-5} \text{ g mm m}^{-2}$  with the addition of cottonseed hydrolysates in alginate films.<sup>33</sup> Another study showed a similar increase from  $2.2 \times 10^{-8} \text{ g mm h}^{-1} \text{ cm}^{-2} \text{ Pa}^{-1}$  to  $3.3 \times 10^{-8} \text{ g mm h}^{-1} \text{ cm}^{-2} \text{ Pa}^{-1}$  when hydrolysate from giant squid was impregnated in gelatin films.<sup>42</sup>

**3.2.5 Transparency and opacity.** Transparency and opacity are essential in film development as they affect the appearance and the consumer's perception.<sup>43</sup> Transparency and opacity are inversely related to each other. It was observed that the transparency decreased from F1 ( $5.5 \pm 0.017\%$ ) to F4 ( $4.4 \pm 0.02\%$ ), and the opacity of the film increased from F1 ( $0.3 \pm 0.001\%$ ) to F4 ( $0.5 \pm 0.008\%$ ) with an increase in the CBP-PH concentration (Table 1). This phenomenon can be attributed to the increased content of solid peptide particles, which contributes to the more compact matrix and enhances light scattering, thereby reducing transparency and increasing opacity.<sup>44</sup> The increase in opacity acts as an effective light barrier, which helps in protecting food when applied in the form of coatings.<sup>17</sup> The results are corroborated by a study where the transparency decreased when whey proteins were added to SA films.<sup>36</sup> Similarly, another reported an increase in opacity from 0.56 to 0.7% with an increase in the silver carp PHs incorporated with fish gelatin films.<sup>45</sup>

**3.2.6 Antioxidant properties.** The F4 film with 2% CBP-PHs showed the highest AA of  $53 \pm 0.75\%$ , while the F3 (1.5% CBP-PHs), F2 (1% CBP-PHs), and F1 (0% CBP-PHs) films showed values of  $48 \pm 0.6$ ,  $42 \pm 0.7$ , and  $39 \pm 0.3\%$ , respectively, against DPPH (Table 2). Film F4 demonstrated the highest AA against an MCA of  $44.5 \pm 0.7\%$  followed by F3  $36.4 \pm 0.5\%$ , F2  $31.1 \pm 0.2\%$ , and F1  $21.3 \pm 0.4\%$ . Similarly, F4 was observed to have the highest HRSA of  $48.5 \pm 0.5\%$  and the lowest was observed in

F1, at  $24.1 \pm 0.2\%$ . This was due to the hydrolysis of CBPs, forming CBP-PHs, which are lower-molecular-weight peptides. The lower molecular weight of peptides possessing antioxidant capacity plays a crucial role in the antioxidant properties of the developed films.<sup>13,46</sup> These peptides exhibit strong radical-scavenging activity, inhibit lipid oxidation, and can effectively chelate metal ions.<sup>47</sup> Similar results were observed when polyvinyl alcohol was impregnated with 6% chicken feather PHs, increasing AA by 23%.<sup>38</sup> Another study also showed an increase in antioxidant properties from 8 to 46% with the increased concentration of fish gelatin films incorporated with silver carp PHs.<sup>45</sup>

**3.2.7 Antibacterial activity.** The antibacterial properties of F1 to F4 films were investigated through inhibition zone assays against *Staphylococcus aureus* (ATCC 25923) and *Klebsiella pneumoniae* (ATCC 13883) (Table 3). Against *S. aureus*, the F4 film demonstrated the largest ZOI of  $24.5 \pm 0.16 \text{ mm}$ , followed by F3 ( $16.4 \pm 0.24 \text{ mm}$ ) and F2 ( $5.8 \pm 0.12 \text{ mm}$ ), and no ZOI was observed in the F1 control film. Similarly, the F4 film exhibited  $21.1 \pm 0.12 \text{ mm}$  against *K. pneumoniae*, followed by F3 ( $15.7 \pm 0.12 \text{ mm}$ ) and F2 ( $5.1 \pm 0.16 \text{ mm}$ ), while F1 again showed no visible ZOI. The antibacterial activity of CBP-PHs was attributed to the small peptides that penetrate the cell wall, altering the bacterial plasma membrane structure. The disruption of the plasma membrane facilitates the entry of the peptide into the bacterium, impacting replication, transcription, and translation, ultimately leading to bacterial death. This was attributed to the electrostatic interactions between the plasma membrane

Table 3 Antibacterial properties of the developed films<sup>a</sup>

Films	Antibacterial properties (mm)	
	<i>Staphylococcus aureus</i>	<i>Klebsiella pneumoniae</i>
F1	Not detected	Not detected
F2	$5.77 \pm 0.12^a$	$5.1 \pm 0.16^a$
F3	$16.4 \pm 0.24^b$	$15.67 \pm 0.12^b$
F4	$24.5 \pm 0.16^c$	$21.07 \pm 0.12^c$

<sup>a</sup> F1, P + SA; F2, P + SA + 1%CBP-PHs; F3, P + SA + 1.5%CBP-PHs; and F4, P + SA + 2%CBP-PHs. P, pectin; SA, sodium alginate; CBP-PHs, chicken byproducts protein hydrolysates. All data are averages of three measurements and reported as mean ± standard deviation (SD). Different letters (a, b, and c) indicate significant differences between groups at  $p < 0.05$  according to Tukey's HSD test.



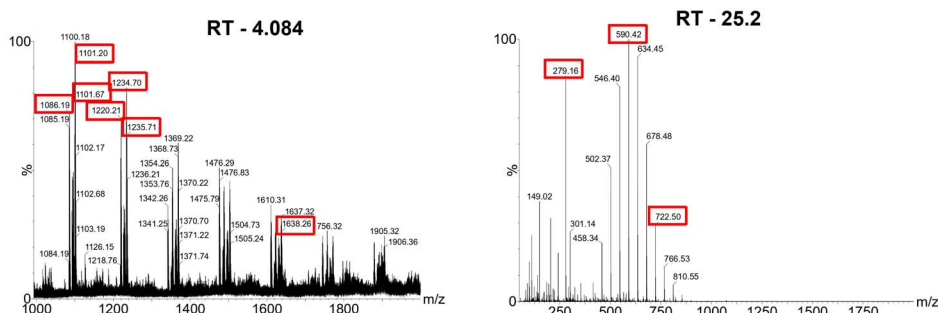


Fig. 2 Identification of bioactive peptides of chicken byproducts protein hydrolysates (CBP-PHs) detected using a Quadrupole-Time-of-Flight High-Resolution Mass Spectrometry (QToF HRMS) system with a  $m/z$  ratio ranging from 100 to 2000.

of the bacteria and the bioactive peptides present in CBP-PHs.<sup>10,34,48</sup> The inhibitory effect of *S. aureus* was greater than that of *K. pneumoniae* due to the additional protective cell layer in the Gram-negative bacteria. This membrane protects the bacteria from environmental stress and regulates the entry of chemicals into the cell.<sup>34,49</sup> This might also explain the increase in the ZOI with an increase in the CPB-PH concentration. The findings of this study align with previous research studies in which PHs derived from Argentine croaker muscle using Alcalase and Protamex showed notable inhibition zones against several bacterial strains.<sup>50</sup> In another study, a wild almond protein isolate was incorporated into Persian gum films, showing a ZOI of 16 and 26 mm for 0.3 and 0.6% (w/v) PHs against *S. aureus*.<sup>35</sup>

**3.2.8 Liquid chromatography-mass spectrometry (LC-MS).** LC-MS of CBP-PHs was conducted to identify the bioactive peptides responsible for their antioxidant and antibacterial properties in the film formulation. The identification of these bioactive sequences confirms the successful hydrolysis of proteins into short-chain peptides with significant functional roles. The presence of lower molecular weight amino acids in CBP-PHs may contribute to the radical scavenging ability of the developed films. The LC-MS spectra demonstrated distinct mass-to-charge ( $m/z$ ) peaks corresponding to the identified peptides, validating their molecular weights and confirming their presence in the hydrolyzed matrix. LC-MS analysis of the CBP-PH sample revealed the presence of several bioactive peptides with potential bioactive properties. The identified peptides included LKA, EDRMSLVDSRCQEA, PDLVF, APGAPGPVG, AR, GIL, LF, IGL, YQKFPQYL, VYFPFGLPN, LAPSLPGKPKPD, DAACAAHCLFRG, LMSYMWSTSM, and LAGNPHQQQN (Table S1 and Fig. S1). These peptides are known to contribute to the antibacterial, antioxidant, and ACE inhibitor activities observed in the formulated films. Among them, the peptide EDRMSLVDSRCQEA, corresponding to Cystatin S (108-121), has been associated with strong antibacterial potential (Fig. 2).<sup>51</sup> Similarly, PDLVF and APGAPGPVG were recognized in earlier studies for their antioxidant potential, which contributes to the radical scavenging ability of the developed films (Fig. 2). The identification of these bioactive sequences confirms the successful hydrolysis of proteins into short-chain peptides with significant functional roles.<sup>52</sup> The presence of such multifunctional peptides supports the

observed enhancement in the film's bioactivity, indicating that enzymatic hydrolysis effectively liberated bioactive fragments responsible for the antimicrobial and antioxidant functionalities of the composite coating.

**3.2.9 Fourier transform infrared (FTIR) spectroscopy.** The FTIR spectrum of the pectin and SA-based films exhibited characteristic absorption bands confirming the presence of functional groups inherent to both polysaccharides (Fig. 3). A broad and intense band at around  $3298\text{ cm}^{-1}$  was observed, corresponding to the stretching vibrations of hydroxyl ( $-\text{OH}$ ) groups, a feature typical of polysaccharide matrices due to

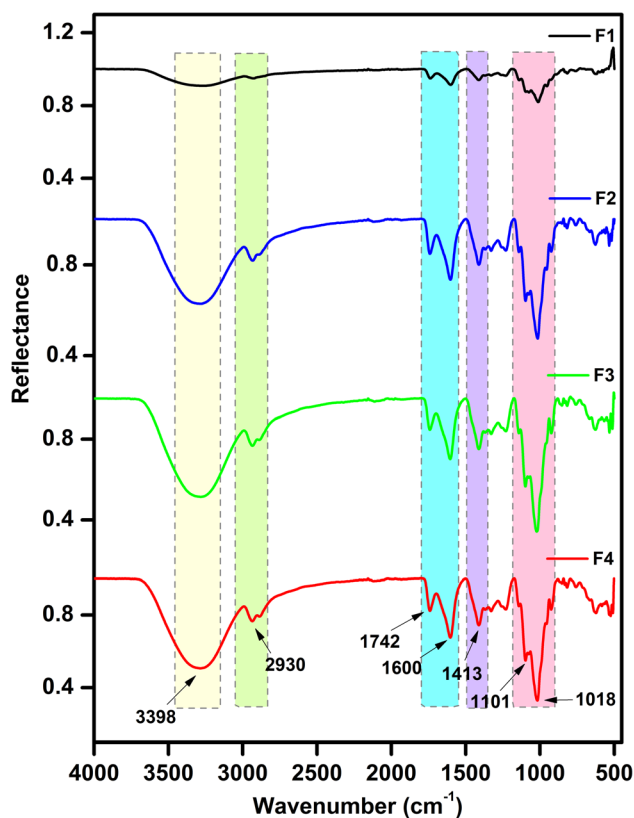


Fig. 3 Fourier transform infrared (FTIR) spectra of the prepared films. F1, P + SA; F2, P + SA + 1%CBP-PHs; F3, P + SA + 1.5%CBP-PHs; and F4, P + SA + 2%CBP-PHs. P, pectin; SA, sodium alginate; CBP-PHs, chicken byproducts protein hydrolysates.





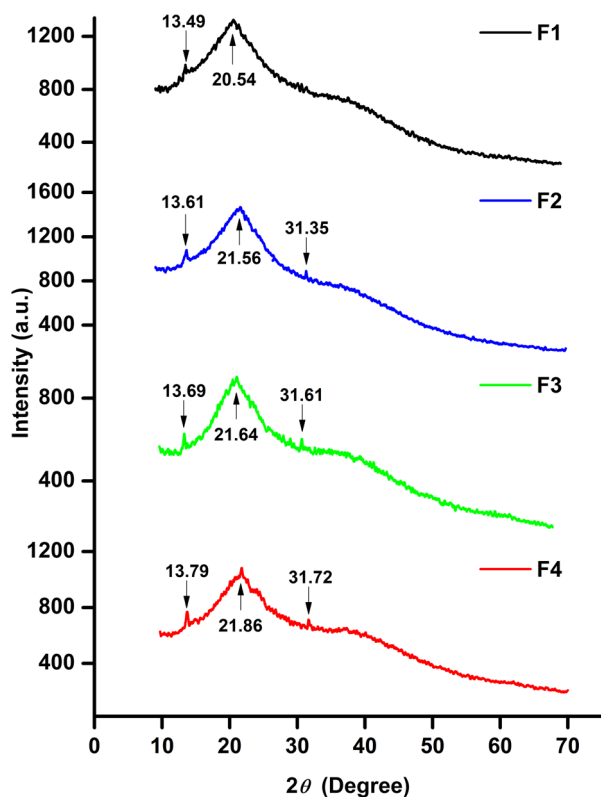


Fig. 4 X-ray diffraction (XRD) patterns of the developed films. F1, P + SA; F2, P + SA + 1%CBP-PHs; F3, P + SA + 1.5%CBP-PHs; and F4, P + SA + 2%CBP-PHs. P, pectin; SA, sodium alginate; CBP-PHs, chicken byproducts protein hydrolysates.

extensive hydrogen bonding.<sup>53</sup> Another prominent peak near 1600 and 1742  $\text{cm}^{-1}$  was attributed to the asymmetric stretching of carboxylate ( $-\text{COO}^-$ ) groups, confirming the presence of uronic acids from alginate and galacturonic acid units from pectin.<sup>54,55</sup> Peaks at around 1413  $\text{cm}^{-1}$  further supported symmetric  $\text{COO}^-$  stretching, while bands near 1018  $\text{cm}^{-1}$  were indicative of C–O–C stretching vibrations associated with glycosidic linkages within the backbone of both polymers.<sup>55,56</sup> These spectral features are consistent with previous FTIR analyses of pectin and SA composites reported in the literature, indicating a strong intermolecular hydrogen bonding that contributes to the structural integrity of the composite film.<sup>57,58</sup>

In the films containing CBP-PHs, intensified peaks were observed at 3398  $\text{cm}^{-1}$  (amide A, N–H stretching), 2930  $\text{cm}^{-1}$  ( $\text{CH}_2$  stretching), and 1600  $\text{cm}^{-1}$  (amide I, C=O vibration). A prominent peak was observed at 1413  $\text{cm}^{-1}$  (amide II, C–N elongation and N–H stretching), while peaks observed at 1101  $\text{cm}^{-1}$  and 1018  $\text{cm}^{-1}$  corresponded to the symmetric and asymmetric stretching of S–O, which could be due to the presence of cysteine bonded by disulphide bridges (the composition of keratin in chicken feathers).<sup>38</sup> These spectral observations support previous findings on protein–polysaccharide blend films, indicating strong biochemical interactions and compatibility between the CBP-PHs and the pectin and SA matrix.<sup>10,38,59</sup>

**3.2.10 X-ray diffraction (XRD).** The XRD pattern was used to study the crystallinity of the developed films (Fig. 4). The

control film, composed of SA and pectin, exhibited characteristic diffraction peaks at approximately 13° and 20°, characteristic of polysaccharide matrices. This was consistent with the previous studies on SA and pectin.<sup>60,61</sup> Incorporating CBP-PHs into the pectin and SA matrix led to subtle changes in the XRD pattern. A prominent diffraction peak was observed at 31° for the CBP-PH films. The relative crystallinity increases with the addition of CBP-PHs. Similar peaks at 13.67, 21.49, and 30.92° were observed in a study using SA and fish PHs generated with *Bacillus siamensis* F2 protease.<sup>17</sup> Similarly, a peak at 32° was observed when 15% garden cress seed PHs produced using alcalase were analyzed.<sup>62</sup>

**3.2.11 Pearson's correlation.** Based on the Pearson correlation analysis of the formulated films (F1–F4), strong correlations were observed among the physicochemical and functional properties (Table S2). AA exhibited a strong positive correlation with density and opacity, indicating that denser and more opaque films possess higher antioxidant potential. Conversely, moisture content and swelling index showed strong negative correlations with AA and density, suggesting reduced water affinity and increased hydrophobicity of the film matrices. Furthermore, the antibacterial activities against *Staphylococcus*

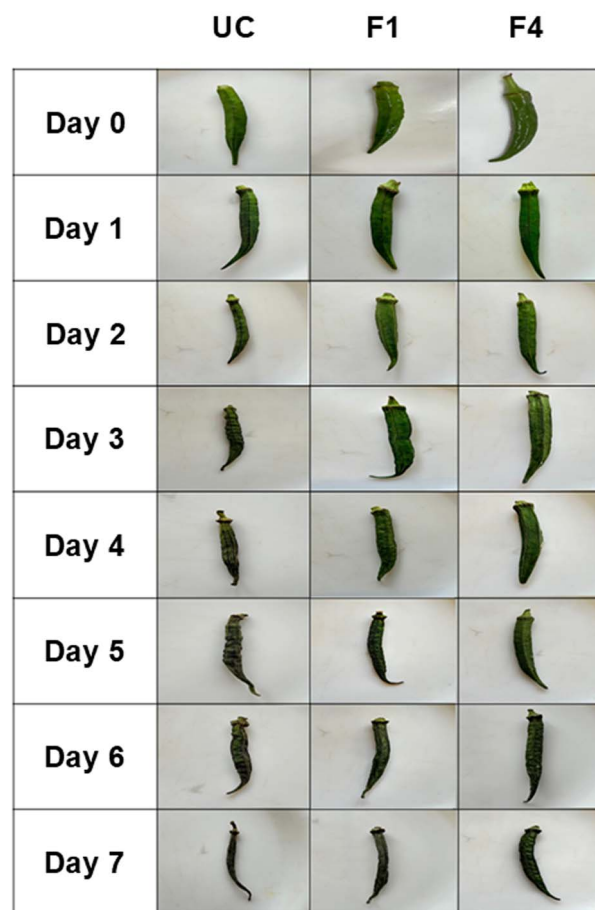


Fig. 5 Effect of storage period (7 days) on uncoated (UC) and coated (F1, P + SA and F4, P + SA + 2%CBP-PHs) okra at room temperature. P, pectin; SA, sodium alginate; CBP-PHs, chicken byproducts protein hydrolysates.



*aureus* and *Klebsiella pneumoniae* correlated positively with the AA, implying that the presence of CBP-PHs enhanced both antioxidant and antimicrobial functionalities. Overall, these correlations confirm that incorporating CBP-PHs into the pectin and SA matrix improves the film's compactness, increases hydrophobicity, and enhances its bioactive properties.

### 3.3 Shelf life studies of the developed films on okra

To evaluate the efficacy of the bioactive films in preserving the quality of okra during a storage period of 7 days, three representative groups were selected for comparative analysis: uncoated, F1-coated (P + SA without CBP-PHs), and F4-coated (P + SA + 2%CBP-PHs) (Fig. 5). This selection was made to establish a clear contrast between the untreated sample, a base composition without bioactive compounds, and the best formulation.

**3.3.1 Weight loss.** Weight loss is linked to texture modification, surface shrivelling, and loss of gloss and nutrients and negatively impacts food quality and shelf life.<sup>22</sup> On day 7 of storage, the uncoated okra showed the maximum weight loss

( $87 \pm 0.29\%$ ) when compared to F1 ( $84 \pm 0.5\%$ ) and F4 ( $78 \pm 0.4\%$ ) (Fig. 6a). This suggests that the presence of a coating acts as a barrier, thus minimizing water loss and respiration, which retains the firmness and membrane integrity of the okra.<sup>31</sup> Moreover, bioactive peptides (CBP-PHs) in F4 coating reduce the growth of microorganisms, further preventing the weight loss of F4-coated okra.<sup>10</sup> A similar observation was reported in a study where coated okra incorporated with chitosan and crude bioactive algae extract from *Spirogyra* sp. showed a lower weight loss compared to the uncoated okra when stored at 27 °C by day 5 of storage.<sup>30</sup>

**3.3.2 pH.** The acidity of okra increased when stored for 7 days at 30 °C (Fig. 6b). The pH of the uncoated samples reduced from  $6.76 \pm 0.03$  to  $5.75 \pm 0.03$  and F1 reduced from  $6.73 \pm 0.06$  to  $6.17 \pm 0.03$ ; however, F4-coated okras maintained their pH by day 7 ( $6.78 \pm 0.05$  to  $6.35 \pm 0.04$ ). The pH of the samples decreased due to the increase in total acids, which in turn increased the hydrogen ion concentration of the okra.<sup>63</sup> The results are in corroboration with a study where the pH of uncoated okra reduced from 6.9 to 5.5, and low density polyethylene (LDPE) maintained the pH at 6.5 for 28 days when stored at 10 °C.<sup>26</sup> A similar decrease in pH with the increase in

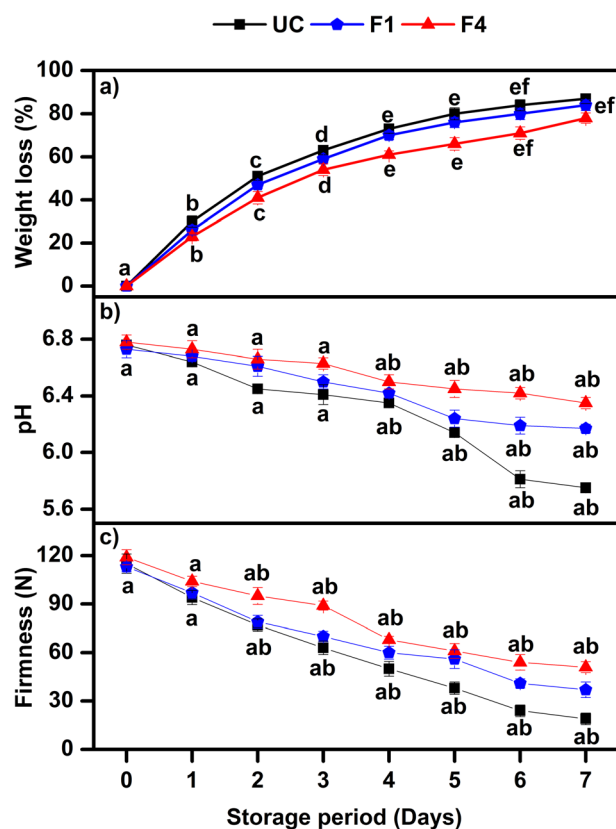


Fig. 6 Study of shelf life parameters of okra. (a) Weight loss, (b) pH, and (c) firmness of uncoated (UC) and coated (F1, P + SA and F4, P + SA + 2%CBP-PHs) after 7 days of storage at room temperature. All data are averages of three measurements and reported as mean  $\pm$  standard deviation (SD). Different letters (a, b, c, d, e, and f) indicate significant differences between groups at  $p < 0.05$  according to the Bonferroni test. P, pectin; SA, sodium alginate; CBP-PHs, chicken byproducts protein hydrolysates.

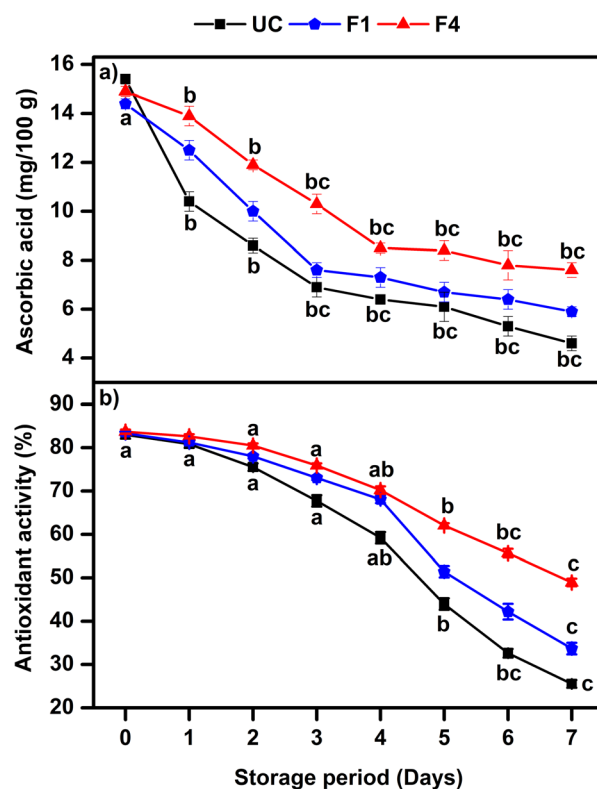


Fig. 7 Study of shelf life parameters of okra. (a) Ascorbic acid and (b) antioxidant activity of uncoated (UC) and coated (F1, P + SA and F4, P + SA + 2%CBP-PHs) after 7 days of storage at room temperature. All data are averages of three measurements and reported as mean  $\pm$  standard deviation (SD). Different letters (a, b, and c) indicate significant differences between groups at  $p < 0.05$  according to the Bonferroni test. P, pectin; SA, sodium alginate; CBP-PHs, chicken byproducts protein hydrolysates.



the storage period was observed in a study when okra was wrapped in LDPE bags.<sup>63</sup>

**3.3.3 Firmness.** Firmness serves as a key indicator of quality and freshness, where its decline signifies the onset of cellular membrane degradation and spoilage, which is correlated with weight loss.<sup>26,64</sup> By day 7, the firmness decreased from  $119 \pm 2.06$  to  $51 \pm 0.78$  N in F4-coated samples,  $113 \pm 1.73$  to  $37 \pm 0.35$  N in F1-coated samples, and  $115 \pm 1.81$  to  $19 \pm 0.35$  N in uncoated okra (Fig. 6c). The firmness is affected by the turgor pressure of the cell and the strength of the cell wall. Enzymatic degradation of cellular components causes the decay of tissues, leading to the breakdown of organic substances and the softening of fruits and vegetables. Coatings act as semi-permeable membranes that decrease the respiration rate of fruits and vegetables, thereby protecting against losses due to oxidation during the storage period of okra.<sup>8,27</sup> Similarly, in a study, the firmness decreased from 173 to 77 N by day 4 of storage when okra was coated with almond and guar gum.<sup>27</sup>

**3.3.4 Ascorbic acid.** Ascorbic acid loss is a reliable indicator of spoilage in okra, as it demonstrates the nutritional loss and oxidative degradation during storage. It is sensitive to temperature, light, oxygen, and storage periods.<sup>25,65</sup> The ascorbic acid content reduces with the increase in the storage period from  $15 \pm 0.21$  mg/100 g to  $4.6 \pm 0.29$  (uncoated okra),  $5.9 \pm 0.22$  (F1-coated okra), and  $7.6 \pm 0.1$  mg/100 g (F4-coated okra) (Fig. 7a). This decrease is attributed to the enzyme ascorbate oxidase that converts ascorbic acid to dehydroascorbic acid.<sup>26,66</sup> A similar reduction in ascorbic acid from 12 to 9.6 mg/100 g was

observed in a study where okra was packed in LDPE packaging.<sup>26</sup>

**3.3.5 Antioxidant activity.** The AA serves as an important indicator of the oxidative stability and freshness of okra, as okra is naturally rich in antioxidant compounds. A gradual decline in AA was observed over a 7-day storage period, indicating progressive oxidative degradation. It was observed that there was a reduction in the AA with each day. By day 7, the AA of okra decreased from  $83 \pm 0.87\%$  to  $25 \pm 0.87\%$  in uncoated okra,  $83 \pm 0.5\%$  to  $34 \pm 1.32\%$  in F1-coated okra and  $84 \pm 0.87\%$  to  $48 \pm 0.87\%$  in F4-coated okra (Fig. 7b). The presence of coating solutions (F1 and F4) acts as a barrier and extends the shelf life of okra when compared to the uncoated okra. CBP-PHs possess antioxidant and antimicrobial activity, which further retains the AA and prevents the growth of microbes, thereby enhancing the shelf life of okra.<sup>10,48,67</sup> A similar reduction in the AA was observed in a study where the AA of okra decreased from 62 to 49.5% in methylenecyclopropene-treated samples. In comparison, it was reduced to 41% in the control samples.<sup>68</sup>

**3.3.6 Color.** During the storage period, shrivelling and browning (darkening) of the ridges negatively impact the appearance of okra. A higher value of  $L^*$  represents whiteness, and a lower value represents blackness. The value of  $a^*$  indicates greenness (negative) or redness (positive), and  $b^*$  indicates blueness (negative) or yellowness (positive).<sup>31</sup> The  $L^*$  value representing lightness decreases with the increase in the storage period from day 0 to 7. By day 7, the  $L^*$  of F4-coated okra reduced from  $34 \pm 0.7$  to  $24 \pm 0.1$ ; however, F1-coated okra reduced from  $34 \pm 0.2$  to  $18 \pm 0.1$ , and uncoated okra reduced

Table 4 Color analysis of the developed coatings on okra after a storage period of 7 days<sup>a</sup>

Films	Storage period (days)	$L^*$	$a^*$	$b^*$	Browning index (BI)
UC	0	$33.3 \pm 0.2^a$	$-4.9 \pm 0.04^a$	$14.9 \pm 0.06^a$	$44.9 \pm 0.7^a$
	1	$28.9 \pm 0.1^a$	$-4.6 \pm 0.01^a$	$14.5 \pm 0.02^a$	$55.4 \pm 0.2^a$
	2	$26.2 \pm 0.1^{ab}$	$-4.1 \pm 0.13^a$	$14.3 \pm 0.02^{ab}$	$61.5 \pm 0.3^a$
	3	$24.8 \pm 0.1^{ab}$	$-3.5 \pm 0.01^{ab}$	$14.1 \pm 0.02^{ab}$	$67.5 \pm 0.2^a$
	4	$23.8 \pm 0.1^{ab}$	$-3.1 \pm 0.02^{ab}$	$13.8 \pm 0.1^{ab}$	$70.5 \pm 0.2^a$
	5	$19.2 \pm 0.1^{ab}$	$-2.6 \pm 0.06^{ab}$	$13.5 \pm 0.2^{ab}$	$98.9 \pm 0.6^{ab}$
	6	$16.4 \pm 0.1^{ab}$	$-2.1 \pm 0.02^{ab}$	$13.2 \pm 0.1^c$	$126.9 \pm 0.4^{ab}$
F1	7	$15.4 \pm 0.1^{ab}$	$-1.8 \pm 0.02^{ab}$	$12.9 \pm 0.4^d$	$139 \pm 0.1^{ab}$
	0	$34.5 \pm 0.2^a$	$-5.0 \pm 0.05^a$	$14.8 \pm 0.5^a$	$44.5 \pm 0.5^a$
	1	$30.4 \pm 0.1^a$	$-4.8 \pm 0.05^a$	$14.6 \pm 0.1^a$	$49.4 \pm 0.1^a$
	2	$28.8 \pm 0.3^{ab}$	$-4.5 \pm 0.06^a$	$14.4 \pm 0.2^{ab}$	$53.4 \pm 1.1^a$
	3	$27.4 \pm 0.1^{ab}$	$-4.1 \pm 0.01^{ab}$	$14.3 \pm 0.4^{ab}$	$57.5 \pm 0.1^a$
	4	$26.8 \pm 0.1^{ab}$	$-3.5 \pm 0.04^{ab}$	$14.1 \pm 0.4^{ab}$	$60.6 \pm 0.3^a$
	5	$23.8 \pm 0.6^{ab}$	$-3.1 \pm 0.01^{ab}$	$13.9 \pm 0.4^{ab}$	$71.5 \pm 0.3^{ab}$
F4	6	$19.1 \pm 0.1^{ab}$	$-2.4 \pm 0.05^{ab}$	$13.5 \pm 0.1^c$	$99 \pm 0.3^{ab}$
	7	$17.7 \pm 0.1^{ab}$	$-2.1 \pm 0.04^{ab}$	$13.1 \pm 0.1^d$	$113.9 \pm 0.9^{ab}$
	0	$33.9 \pm 0.7^a$	$-5 \pm 0.3^a$	$14.8 \pm 0.5^a$	$44.8 \pm 0.5^a$
	1	$31.1 \pm 0.5^a$	$-4.9 \pm 0.06^a$	$14.7 \pm 0.1^a$	$48.3 \pm 0.5^a$
	2	$30.4 \pm 0.1^{ab}$	$-4.7 \pm 0.02^a$	$14.5 \pm 0.2^{ab}$	$49.4 \pm 0.2^a$
	3	$29.1 \pm 0.6^{ab}$	$-4.4 \pm 0.07^{ab}$	$14.4 \pm 0.4^{ab}$	$53 \pm 0.9^a$
	4	$28.8 \pm 0.3^{ab}$	$-4.1 \pm 0.01^{ab}$	$14.3 \pm 0.4^{ab}$	$53.8 \pm 0.2^a$
5	$26.3 \pm 0.1^{ab}$	$-3.8 \pm 0.01^{ab}$	$14 \pm 0.3^{ab}$	$60.5 \pm 0.3^{ab}$	
6	$24.8 \pm 0.1^{ab}$	$-3.1 \pm 0.01^{ab}$	$13.7 \pm 0.1^c$	$66.1 \pm 0.4^{ab}$	
7	$23.9 \pm 0.1^{ab}$	$-2.5 \pm 0.08^{ab}$	$13.4 \pm 0.1^d$	$72 \pm 0.4^{ab}$	

<sup>a</sup> UC, uncoated okra; F1, P + SA, and F4, P + SA + 2%CBP-PHs. P, pectin; SA, sodium alginate; CBP-PHs, chicken byproducts protein hydrolysates. All data are averages of three measurements and reported as mean  $\pm$  standard deviation (SD). Different letters (a, b, c, and d) indicate significant differences between groups at  $p < 0.05$  according to the Bonferroni test.



from  $33 \pm 0.2$  to  $15 \pm 0.1$  (Table 4). Similarly, the  $a^*$  value increased from  $-5 \pm 0.3$  to  $-2.5 \pm 0.08$  in F4-coated,  $-5 \pm 0.05$  to  $-2.1 \pm 0.04$  in F1-coated, and  $-4.9 \pm 0.04$  to  $-1.8 \pm 0.02$  in uncoated okra. The  $b^*$  value decreased from  $14.8 \pm 0.5$  to  $13.4 \pm 0.1$  in F4-coated okra,  $14.8 \pm 0.5$  to  $13.1 \pm 0.1$  in F1-coated okra, and  $14.9 \pm 0.06$  to  $12.9 \pm 0.4$  in the uncoated okra. The  $L^*$  of okra decreased due to the darkening of ridges, the  $a^*$  increased due to the loss of the green color of the okra, and the  $b^*$  decreased due to the discoloration of okra with the increase in the storage period.<sup>31</sup> These results indicate that the F4-coating preserved the color of okra better than the F1-coated and uncoated okra, which suggests the efficacy of CBP-PHs in maintaining the visual appeal of okra during the storage period. A similar trend was observed in okra with SA-coating, using basil oil nano-emulsified with Tween 20, where the  $L^*$  value decreased from 41.1 to 30.6 in uncoated okra, while the coated okra observed a decrease from 40.5 to 33.5 by day 3 of storage at 24 °C. In the same study, the  $a^*$  value increased from  $-8.2$  to  $-6.4$  in the uncoated okra, while the coated okra preserved the  $a^*$  value ( $-8.1$  to  $-6.7$ ).<sup>31</sup> Similarly, in another study, on day 7, when okra was coated with guar gum, almond gum, and oregano oil, the  $b^*$  value decreased from 9.1 to 8.4, and in the control okra, it decreased from 9.1 to 7.5.<sup>27</sup>

The BI indicates the quality of fruits and vegetables, such as apples, avocados, and okra.<sup>31</sup> The BI increased from  $45 \pm 0.5$  to  $72 \pm 0.4$  in F4-coated okra and  $44 \pm 0.5$  to  $114 \pm 0.9$  in F1-coated okra, and the highest increase was observed in uncoated okra, from  $45 \pm 0.7$  to  $139 \pm 0.1$  (Table 4). The BI increased due to the darkening of the ridges, resulting in discoloration of the okra with an increase in the storage period.<sup>31</sup> The results are in corroboration with an increase in the BI from 85 to 144 in the coated okra using SA impregnated with basil oil nano-emulsified with Tween 20 by day 3 of storage at 24 °C and from 83 to 189 in the control.<sup>31</sup>

**3.3.7 Total chlorophyll content.** Chlorophyll loss during storage is a key indicator of senescence, which is driven by the enzyme chlorophyllase.<sup>26</sup> The uncoated samples lost the maximum amount of chlorophyll ( $13.4 \pm 0.11$  to  $4 \pm 0.09$  mg/100 g), followed by F1-coated okra ( $13.4 \pm 0.04$  to  $5.8 \pm 0.17$  mg/100 g), while the F4-coated okra ( $13.4 \pm 0.07$  to  $8.1 \pm 0.05$  mg/100 g) retained the maximum amount of chlorophyll (Fig. 8). Temperature and pH play an essential role in influencing the stability of chlorophyll during the storage period. The degradation of the chlorophyll pigment increases with temperature (30 °C), while higher pH levels help in retaining chlorophyll more effectively.<sup>69–71</sup> The chlorophyllase enzyme plays a crucial role during senescence as it utilizes chlorophyll a as its substrate, resulting in a visible loss of green color in okra.<sup>26</sup> A similar decline in chlorophyll content was observed in a study where okra was packed in different thicknesses of LDPE packaging.<sup>26</sup> Another study observed a similar decrease in chlorophyll when spinach was coated with whey protein concentrate and rosemary essential oil.<sup>69</sup>

**3.3.8 Total microbial count.** The microbial analysis reveals the growth of organisms during 7 days of storage at 30 °C on okra, which directly affects its shelf life. It was observed that on day 0, the total mesophilic count was  $3.9 \pm 0.02$  log CFU g<sup>-1</sup>,

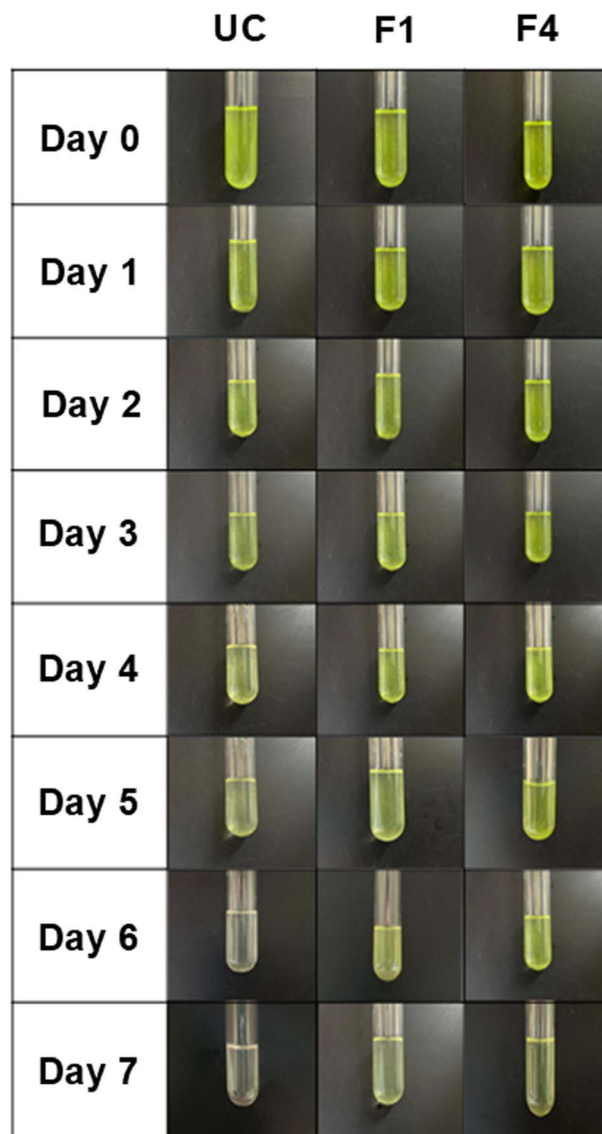


Fig. 8 Effect of the storage period (7 days) on total chlorophyll content of uncoated (UC) and coated (F1, P + SA and F4, P + SA + 2% CBP-PHs) okra at room temperature. P, pectin; SA, sodium alginate; CBP-PHs, chicken byproducts protein hydrolysates.

which increased in all the samples with the increase in the storage period (Fig. 9a). The uncoated samples showed the highest mesophilic count of  $6.3 \pm 0.07$  log CFU g<sup>-1</sup> on day 7, followed by F1-coated okra ( $6 \pm 0.02$  log CFU g<sup>-1</sup>). In contrast, F4-coated exhibited the lowest by maintaining the mesophilic count at  $5.7 \pm 0.03$  log CFU g<sup>-1</sup>. Similarly, by day 7, the count of yeast and mold also increased from  $3.6 \pm 0.02$  log CFU g<sup>-1</sup> (day 0) to  $5.8 \pm 0.05$  log CFU g<sup>-1</sup> in uncoated okra, followed by F1-coated ( $5.5 \pm 0.06$  log CFU g<sup>-1</sup>) and F4-coated okra ( $5.3 \pm 0.01$  log CFU g<sup>-1</sup>) (Fig. 9b). This shows that the F4 coating enhanced the shelf life of okra due to its antimicrobial properties, which effectively suppressed microbial proliferation. The bioactive peptides of CBP-PHs penetrate the microbial cell wall and alter the cell membrane structure, ultimately leading to the



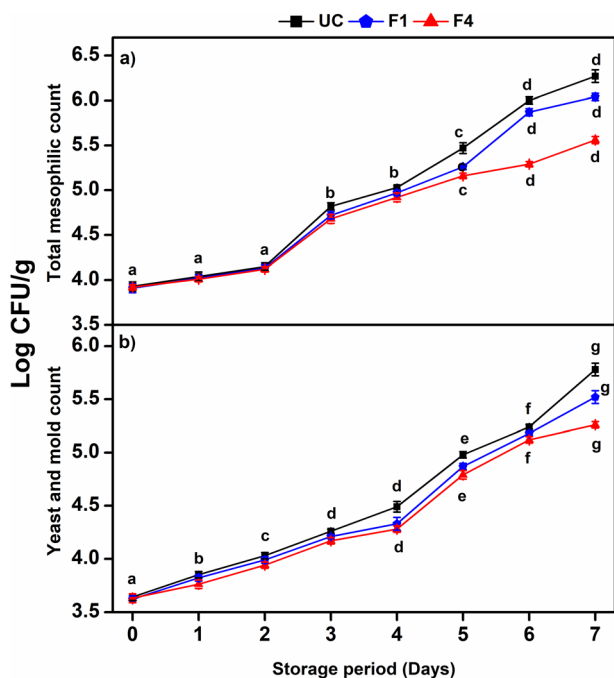


Fig. 9 Effect of storage period (7 days) on microbial growth, (a) total mesophilic count and (b) yeast and mold count of uncoated (UC) and coated (F1, P + SA and F4, P + SA + 2%CBP-PHs) okra at room temperature. All data are averages of three measurements and reported as mean  $\pm$  standard deviation (SD). Different letters (a, b, c, d, e, f, and g) indicate significant differences between groups at  $p < 0.05$  according to the Bonferroni test. P, pectin; SA, sodium alginate; CBP-PHs, chicken byproducts protein hydrolysates.

death of bacterial cells.<sup>10</sup> The results are in corroboration with a study where chitosan and zinc oxide-coated okra samples restricted the bacterial and fungal cells at approximately  $10 \times 10^7$  CFU mL<sup>-1</sup> and  $2 \times 10^7$  CFU mL<sup>-1</sup>, respectively.<sup>72</sup>

## 4 Conclusion

The current study aimed to develop and characterize an active packaging using pectin, SA, and CBP-PHs obtained through enzymatic hydrolysis of CBPs using the protease from *Bacillus stamensis* F2. Among the formulations tested, F4 (P + SA + 2% CBP-PHs) demonstrated enhanced antibacterial properties against *Staphylococcus aureus* ( $24.5 \pm 0.16$  mm) and *Klebsiella pneumoniae* ( $21 \pm 0.12$  mm) and antioxidant (DPPH,  $53 \pm 0.75\%$ ), surface hydrophobicity ( $132^\circ$ ) and optical and physical properties. When this coating was applied to okra, F4 effectively minimized weight loss ( $78 \pm 0.4\%$ ), retained firmness ( $51 \pm 0.8$  N), preserved chlorophyll ( $8.1 \pm 0.05$  mg/100 g) and ascorbic acid content ( $7.6 \pm 0.1$  mg/100 g), and suppressed microbial proliferation during storage. These findings underscore the importance of bioactive CBP-PHs when incorporated into food-grade biopolymers. Beyond material innovation, this study highlights the importance of food preservation through waste valorisation (CBP-PHs from CBPs), thereby addressing food security and sustainability and reducing environmental burden by replacing conventional plastics. Future prospects of the current research include optimizing film formulation for

commercial production and utilising it on various perishable products to extend their shelf life.

## Author contributions

AR: data curation, analysis, writing, and editing of the manuscript. VGP: funding, designing the experiments, data curation, analysis, overall supervision, writing, and editing of the manuscript. AK: data curation, analysis, writing, and editing of the manuscript. SS: data curation, analysis, and editing of the manuscript. MK: data curation and analysis. NS: data analysis and editing of the manuscript.

## Conflicts of interest

The authors declare that there is no conflict of interest.

## Data availability

Additional datasets related to the identification of bioactive peptides and possible correlations between the variables of the films are available.

Supplementary information (SI) is available. See DOI: <https://doi.org/10.1039/d5fb00468c>.

## Acknowledgements

This work was supported by projects: a UGC-BSR Start-up grant with Ref No. No. F. 30-456/2018 (BSR) and GITAM: Research Seed Grants (RSG) Ref No. F. No. 2021/0087. The authors are thankful to the "MURTI" (Multi-disciplinary Unit of Research on Translation Initiative) facility, MURTI-SAIF facility, and the Department of Mechanical Engineering of the Gandhi Institute of Technology and Management for providing instrumental facilities (FTIR, XRD, LC-MS, and the contact angle meter) for conducting experiments required for this article.

## References

- 1 M. P. M. García, M. C. Gómez-Guillén, M. E. López-Caballero and G. V. Barbosa-Cánovas, *Edible Films and Coatings: Fundamentals and Applications*, CRC Press, 2016.
- 2 Y. Zhao, B. Li, C. Li, Y. Xu, Y. Luo, D. Liang and C. Huang, *Foods*, 2021, **10**, 1845.
- 3 C. E. Realini and B. Marcos, *Meat Sci.*, 2014, **98**, 404–419.
- 4 N. Omerović, M. Djisalov, K. Živojević, M. Mladenović, J. Vunduk, I. Milenković, N. Ž. Knežević, I. Gadjanski and J. Vidić, *Compr. Rev. Food Sci. Food Saf.*, 2021, **20**, 2428–2454.
- 5 R. Abka-Khajouei, L. Tounsi, N. Shahabi, A. K. Patel, S. Abdelkafi and P. Michaud, *Mar. Drugs*, 2022, **20**, 364.
- 6 M. G. Kontominas, *Foods*, 2020, **9**, 1440.
- 7 K. Y. Perera, A. K. Jaiswal and S. Jaiswal, *Foods*, 2023, **12**, 2422.
- 8 A. Ramadoss, V. G. Poosarla, S. Sadiya and N. Shivshetty, *J. Food Sci.*, 2025, **90**, e70179.
- 9 J. Tkaczewska, *Trends Food Sci. Technol.*, 2020, **106**, 298–311.



- 10 O. Zinina, S. Merenkova and D. Galimov, *Sustainability*, 2023, **15**, 15086.
- 11 L. O. L. d. Rosa, M. C. Santana, T. L. Avezedo, A. I. S. BRÍGIDA, R. Godoy, S. Pacheco, C. Mellinger-Silva and L. M. C. CABRAL, *Food Sci. Technol.*, 2018, **38**, 31–36.
- 12 D. S. Ningthoujam, P. Kshetri, S. Sanasam and S. Nimaichand, *World Appl. Sci. J.*, 2009, **7**, 907–916.
- 13 B. G. Rathod, V. G. Poosarla, S. K. Kuppili, K. S. Y. R. Chouhan and N. Shivshetty, *Biomass Convers. Biorefin.*, 2024, **14**, 1343–1358.
- 14 S. Sankaralingam, B. Harinathan, S. Palpperumal, D. Kathiresan, S. Rajendran, T. Shankar, D. Prabhu and N. Sivakumar, *Am.–Eurasian J. Agric. Environ. Sci.*, 2017, **17**, 293–299.
- 15 M. Vidyasagar, S. Prakash and K. Sreeramulu, *Lett. Appl. Microbiol.*, 2006, **43**, 385–391.
- 16 X. Chen, D. Jiang, P. Xu, Z. Geng, G. Xiong, Y. Zou, D. Wang and W. Xu, *Food Chem.*, 2021, **343**, 128417.
- 17 S. Sadiya, V. G. Poosarla, A. Ramadoss, B. G. Rathod, N. Shivshetty and G. Rajagopalan, *ACS Food Sci. Technol.*, 2025, **5**, 2820–2832.
- 18 H. F. Gemedé, N. Ratta, G. D. Haki, A. Z. Woldegiorgis and F. Beyene, *J. Food Process. Technol.*, 2015, **6**, 2.
- 19 L. M. R. Gonzales and M. M. Benitez, *Mindanao J. Sci. Technol.*, 2023, **21**, 153–177.
- 20 M. L. Zambrano-Zaragoza, R. González-Reza, N. Mendoza-Muñoz, V. Miranda-Linares, T. F. Bernal-Couoh, S. Mendoza-Elvira and D. Quintanar-Guerrero, *Int. J. Mol. Sci.*, 2018, **19**, 705.
- 21 B. G. Rathod, S. Pandala and V. G. Poosarla, *Appl. Biochem. Biotechnol.*, 2023, **195**, 4775–4795.
- 22 V. G. Poosarla, S. Bisoi, A. Siripurapu, B. G. Rathod, A. Ramadoss, S. Kilaparathi, N. Shivshetty and G. Rajagopalan, *J. Food Sci.*, 2024, **89**, 6232–6252.
- 23 M. Alinejad, H. Shahiri Tabarestani and A. Motamedzadegan, *LWT–Food Sci. Technol.*, 2025, **232**, 118419.
- 24 S. Roytrakul, S. Charoenlappanit, S. Kittisenachai, N. Siangpro, J. Sichaem, S. Chuakrut, S. Sarin and R. Jutakanoke, *PLoS One*, 2024, **19**, e0314482.
- 25 M. R. Zare-Bavani, *J. Food Sci. Technol.*, 2024, **20**, 149–169.
- 26 D. Paulus, S. B. Ferreira and D. Becker, *AIMS Agric. Food.*, 2021, **6**, 321–336.
- 27 M. M. Shinde, M. Malik, K. Kaur, V. K. Gahlawat, N. Kumar, P. Chiraang and A. Upadhyay, *Int. J. Biol. Macromol.*, 2024, **262**, 129630.
- 28 S. Sadasivam, *Biochemical Methods*, New age international, 1996.
- 29 R. Reis, H. Sipahi, O. Dinc, T. Kavaz, M. Charehsaz, A. Dimoglo and A. Aydın, *Hum. Exp. Toxicol.*, 2021, **40**, 452–463.
- 30 S. Soiklom, W. Siri-Anusornsak, K. Petchpoung, S. Soiklom and T. Maneeboon, *Foods*, 2025, **14**, 804.
- 31 G. Gundewadi, S. G. Rudra, D. J. Sarkar and D. Singh, *Food Packag. Shelf Life*, 2018, **18**, 1–12.
- 32 D. I. Arnon, *Plant Physiol.*, 1949, **24**, 1–15.
- 33 J. G. d. Oliveira Filho, J. M. Rodrigues, A. C. F. Valadares, A. B. d. Almeida, T. M. d. Lima, K. P. Takeuchi, C. C. F. Alves, H. A. d. F. Sousa, E. R. d. Silva, F. H. Dyszy and M. B. Egea, *Food Hydrocolloids*, 2019, **92**, 267–275.
- 34 P. Raei, M. Khomeiri, A. S. Mahounak, A. Moayedi and M. Kashiri, *Appl. Food Res.*, 2025, **5**, 100727.
- 35 Z. Tahsiri, S. Hedayati and M. Niakousari, *Food Hydrocolloids Health*, 2025, 100199.
- 36 S. Bishnoi, J. Trifol, R. Moriana and A. C. Mendes, *Food Chem.*, 2022, **391**, 133196.
- 37 S. Kim, H. Lim, S. Park, D.-S. Kim and H. W. Kwak, *Ind. Crops Prod.*, 2025, **225**, 120564.
- 38 M. M. F. Santos, C. V. B. Grisi, D. A. S. Lima, G. I. B. Florentino, V. C. d. S. Ferreira, M. S. Madruga and F. A. P. d. Silva, *Food Biosci.*, 2024, **62**, 105048.
- 39 S. Rbihi, A. Aboulouard, L. Laallam and A. Jouaiti, *Surf. Interfaces*, 2020, **21**, 100708.
- 40 S. Tang, Z. Wang, P. Li, W. Li, C. Li, Y. Wang and P. K. Chu, *Nanomaterials*, 2018, **8**, 930.
- 41 T. Dursun Capar, *Food Packag. Shelf Life*, 2023, **37**, 101068.
- 42 B. Giménez, J. Gómez-Estaca, A. Alemán, M. C. Gómez-Guillén and M. P. Montero, *Food Hydrocolloids*, 2009, **23**, 1322–1327.
- 43 H. M. S. Akhtar, A. Riaz, Y. S. Hamed, M. Abdin, G. Chen, P. Wan and X. Zeng, *Int. J. Biol. Macromol.*, 2018, **118**, 469–477.
- 44 C. Chang and M. T. Nickerson, *Food Sci. Technol. Int.*, 2015, **21**, 33–44.
- 45 A. Hasanzati Rostami, A. Motamedzadegan, S. E. Hosseini, M. Rezaei and A. Kamali, *J. Aquat. Food Prod. Technol.*, 2017, **26**, 457–467.
- 46 M. M. F. Santos, C. V. B. Grisi, E. G. T. de Souza, J. d. M. Lima, V. C. d. S. Ferreira, L. E. Kurozawa, M. S. Madruga and F. A. P. da Silva, *Food Biosci.*, 2024, **59**, 103897.
- 47 M. Nikoo, J. M. Regenstein and M. Yasemi, *Foods*, 2023, **12**, 4470.
- 48 P. Andiana, M. G. M. Syahdan, A. H. Utama, K. Kasri, K. U. Al Awwaly and A. Manab, *J. Ilmu dan Teknol. Has. Ternak.*, 2024, **19**, 15–24.
- 49 P. Castellano, L. Mora, E. Escudero, G. Vignolo, R. Aznar and F. Toldrá, *Food Microbiol.*, 2016, **59**, 133–141.
- 50 M. Da Rocha, A. Alemán, V. P. Romani, M. E. López-Caballero, M. C. Gómez-Guillén, P. Montero and C. Prentice, *Food Hydrocolloids*, 2018, **81**, 351–363.
- 51 M. F. Blankenvoorde, W. Van't Hof, E. Walgreen-Weterings, T. Van Steenberghe, H. Brand, E. Veerman and A. Nieuw Amerongen, *Biol. Chem.*, 1998, **379**, 1371–1376.
- 52 T. Anna, K. Alexey, B. Anna, K. Vyacheslav, T. Mikhail and M. Ulia, *Curr. Res. Nutr. Food Sci.*, 2016, **4**, 77–86.
- 53 N. Thombare, A. Mahto, D. Singh, A. R. Chowdhury and M. F. Ansari, *J. Polym. Environ.*, 2023, **31**, 3372–3380.
- 54 Z. Mahcene, A. Khelil, S. Hasni, P. K. Akman, F. Bozkurt, K. Birech, M. B. Goudjil and F. Tornuk, *Int. J. Biol. Macromol.*, 2020, **145**, 124–132.



- 55 Y. Roman Maldonado, S. J. Villanueva-Rodríguez, H. M. Hernández-Hernández, E. Terrés and J. Cervantes Martínez, *Foods*, 2024, **13**, 3914.
- 56 S. Azeez and R. Shenbagaraman, in *Characterization Techniques in Bionanocomposites*, ed. S. Ahmed and C. M. Hussain, Woodhead Publishing, United Kingdom, 2025, pp. 209–227.
- 57 M. M. Ahmad, K. Chauhan, A. Naz and M. Nayeem, *Pharma Innovation*, 2021, **10**, 262–272.
- 58 R. Pereira, A. Tojeira, D. C. Vaz, A. Mendes and P. Bártolo, *Int. J. Polym. Anal. Charact.*, 2011, **16**, 449–464.
- 59 A. Bhimrao Muley, A. Bhalchandra Pandit, R. Satishchandra Singhal and S. Govind Dalvi, *Ultrason. Sonochem.*, 2021, **71**, 105385.
- 60 S. Liu, Y. Li and L. Li, *Carbohydr. Polym.*, 2017, **160**, 62–70.
- 61 R. K. Mishra, A. B. A. Majeed and A. K. Banthia, *Int. J. Plast. Technol.*, 2011, **15**, 82–95.
- 62 M. Z. Mulla, J. Ahmed, S. F. Habeebullah and A. Vahora, *J. Food Meas. Char.*, 2022, **16**, 5058–5065.
- 63 G. Babarinde and O. Fabunmi, *Agric. Tropica Subtropica*, 2009, **42**, 151–156.
- 64 S. K. Jha, S. Sethi, M. Srivastav, A. K. Dubey, R. R. Sharma, D. V. K. Samuel and A. K. Singh, *J. Food Eng.*, 2010, **97**, 208–212.
- 65 A.-H. A. H. El-Shaieny, N. A. A. Abd-Elkarim, E. M. Taha and S. Gebril, *Agriculture*, 2022, **12**, 1699.
- 66 F. Adetuyi, A. Osagie and A. Adekunle, *J. Food Technol.*, 2008, **6**, 227–230.
- 67 M. M. F. Santos, C. V. B. Grisi, D. A. S. Lima, G. I. B. Florentino, V. C. da Silva Ferreira, M. S. Madruga and F. A. P. da Silva, *Food Biosci.*, 2024, **62**, 105048.
- 68 R. Kanwal, H. Ashraf, M. Sultan, I. Babu, Z. Yasmin, M. Nadeem, M. Asghar, R. R. Shamshiri, S. M. Ibrahim and N. Ahmad, *Sustainability*, 2020, **12**, 7547.
- 69 A. Abedi, L. Lakzadeh and M. Amouheydari, *J. Food Process. Preserv.*, 2021, **45**, e15284.
- 70 D. Gernah and A. Daagema, *Curr. Res. J. Biol. Sci.*, 2012, **4**, 444–448.
- 71 P. Nisha, R. S. Singhal and A. B. Pandit, *J. Food Eng.*, 2004, **64**, 135–142.
- 72 L. Al-Naamani, J. Dutta and S. Dobretsov, *Nanomaterials*, 2018, **8**, 479.

